J Mater Sci (2010) 45:2150–2156
DOI 10.1007/s10853-009-3909-6

HTC2009

Wetting dynamics versus interfacial reactivity of AlSi alloys on carbon

N. R. Calderon · R. Voytovych · J. Narciso · N. Eustathopoulos

Received: 15 June 2009 / Accepted: 17 September 2009 / Published online: 30 September 2009

Abstract The wetting dynamics of silicon carbide forming AlSi alloys on carbon substrates is studied by the dispensed drop technique in high vacuum by varying the parameters: alloy composition, temperature and type of carbon (vitreous carbon, pyrocarbon and pyrographite). The results on wetting are analysed in relation to those on interfacial reactivity and compared with model predictions.

Introduction

Wetting of ceramics by liquid metals is often promoted using alloying elements which form continuous layers of a better-wetted compound at the interface, by reaction with the ceramic [1]. In wetting experiments, two types of reactivity must be distinguished: reactivity at the solid–liquid–vapour triple line (hereafter referred to as the reactivity at the triple line) and reactivity at the interface behind the triple line (referred to as interfacial reactivity). The reactivity at the triple line is relevant for wetting while the interfacial reactivity has no or only limited effect on wetting dynamics [2]. However, the interfacial reactivity is important for other properties of the metal/ceramic junction, for instance, for its mechanical properties. Indeed, thickening of the reaction layer is often detrimental to the mechanical properties of the system [3].

In this work, the wetting dynamics and interfacial reactivity of AlSi alloys on carbon substrates are studied in high vacuum using the dispensed drop technique. The AlSi/graphite system is a candidate for the processing of metal matrix composites [4] and also presents an interest in processing by liquid phase epitaxy of SiC monocrystals growing from AlSi alloys in contact with a carbon source [5]. In relation with this application, Jacquier et al. [6] performed an extensive study on reactivity for a polycrystalline graphite rod immersed in AlSi alloys for times ranging from 1 to 48 h at 1100 °C under a static Ar pressure. Although our study is for the same system, it involves a different geometry (the alloy/carbon interface is flat) and different contact times (less than 1 h, i.e. times typical of wetting experiments).

For the AlSi/carbon system, it is well established that at any temperature there is a critical value x^*_{Si} of silicon mole fraction in the liquid alloy above which silicon reacts with carbon to form silicon carbide [7]. For alloys more diluted in Si, the system is still reactive but the reaction product formed at the interface is aluminium carbide. In the present study, experiments are performed with two alloys, Al–25 at. %Si and Al–40 at. %Si, at 850 and 1000 °C. For these compositions and temperatures SiC is expected to form at the interface. Note that at temperatures higher than 1000 °C, pollution of the furnace by Al evaporation occurring in high vacuum becomes significant while at temperatures below 850 °C spreading becomes too slow.

N. R. Calderon · J. Narciso
Department de Química Inorgánica, University of Alicante, Apdo. 99, 03080 Alicante, Spain

N. R. Calderon · J. Narciso
Instituto Universitario de Materiales de Alicante, University of Alicante, Apdo. 99, 03080 Alicante, Spain

R. Voytovych · N. Eustathopoulos (✉)
SIMaP/PHELMA, INPG, D.U., BP 75, 38402 St. Martin d'Hères, France
e-mail: nikos@simap.grenoble-inp.fr

Although most of the experiments were carried out with vitreous carbon substrates, two other types of carbon with different densities and microstructures were also used.

Experimental procedure

Wetting was studied by the "dispensed drop" method which is derived from the classical sessile drop technique, in a metallic furnace under a vacuum of 5×10^{-5} Pa. Once the experiment temperature is attained, the liquid is extruded from the crucible and deposited on the substrate surface, then spreading occurs as in the classical sessile drop configuration. In this way, the processes of melting and spreading are separated and fully isothermal experiments can be performed. Note that during extrusion any oxide layer on the liquid surface alloy is broken and remains in the crucible.

The drop images were produced using an optical system fitted with a zoom (magnification of ×30). The wetting process was filmed by a CCD video camera and recorded on videotape at a film speed of 25 frames per second. All contact angles measured are advancing contact angles. After the experiment, contact angle θ and drop base radius R were measured from the drop profile using a drop shape analysis software with an accuracy of ±2° for θ and ±1% for R.

The aluminium–silicon alloys used are prepared in situ from pure Al (99.9997 wt%) and Si (99.9995 wt%) by melting and alloying in an alumina crucible prior to drop deposition.

Vitreous carbon (C_v) substrates of V25 grade, featuring no open porosity, an ash content of less than 50 ppm, a density $\rho = 1.50$–1.55×10^3 kg/m^3 and a graphitisation degree (GD) of 0, were provided by Carbone–Lorraine. Their surface was polished to an average roughness R_a of less than 10 nm. In addition to vitreous carbon two other carbon substrates without open porosity but with different GD (measured by XR-diffraction) and ρ values were studied, namely a pyrolytic carbon denoted PC ($\rho = 2.20 \times 10^3$ kg/m^3, GD = 27%, $R_a = 3$ μm) and a highly oriented pyrolytic graphite, denoted HOPG ($\rho = 2.26 \times 10^3$ kg/m^3, GD = 99%). Note that the HOPG substrate is the commercially available material with the properties closest to monocrystalline graphite. Its average roughness measured on areas of 20×20 μm^2 is 2–4 nm.

After cooling, the specimens were cut perpendicular to the interface. The first half was embedded in resin and polished for optical and SEM observations while on the second part of the specimen, the metal droplet was dissolved using a NaOH solution so as to reveal the interfacial area.

Results and discussion

Spreading kinetics

A typical plot of drop base diameter and contact angle θ versus time for an experiment conducted at 1000 °C with an Al–25 at% Si alloy on vitreous carbon is given in Fig. 1.

The contact angle in this system decreases from high non-wetting contact angles close to 150° to wetting contact angles near 50° in about 10^3 s. This time exceeds by five orders of magnitude the spreading times observed for metallic droplets in non-reactive liquid/solid systems [8–10]. This clearly shows that wetting of C_v by AlSi alloy is controlled by the reaction between Si and carbon and not by viscous dissipation.

Two reactive kinetic stages can be distinguished on the $d(t)$ curve (Fig. 1b). During most of the spreading kinetics (up to the angle $\theta_N \approx 50°$), the spreading rate $U = dR/dt$ decreases continuously (very rapidly during the first 100 s and then much more slowly) and tends to a nearly constant value, noted U^*, in the θ range from about 90° to 50° (Fig. 1b). This fact indicates that the spreading kinetics is not controlled by long-range diffusion of the reactive element (Si), but by the local reaction process at the triple line [11, 12]. The second stage appears abruptly at $\theta = \theta_N$ and is accompanied by a sevenfold decrease in spreading rate. Indeed, a careful examination of the $R(t)$ curve of the experiment presented in Fig. 1 shows that at $\theta < \theta_N$ the spreading rate was very small (0.1 μm/s) but not nil. As argued by Dezellus [13], during this stage the liquid has no direct access to the substrate surface resulting in slow reaction rate. According to [14] the steady contact angle in a

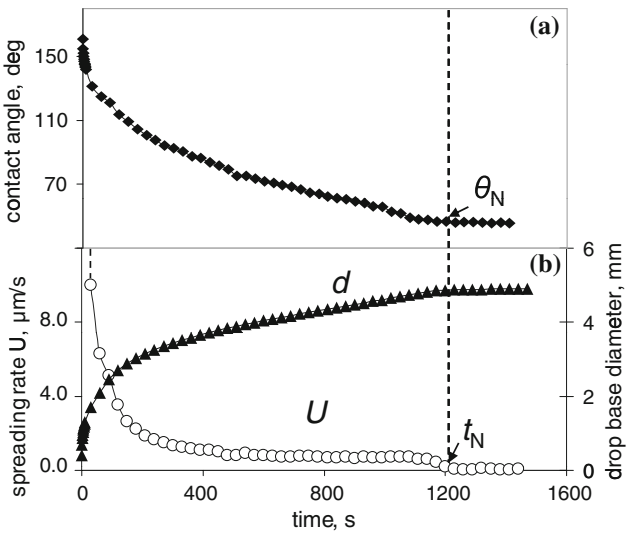

Fig. 1 Contact angle θ, drop base diameter d and spreading rate U versus time for an experiment conducted on vitreous carbon with an Al–25 at% Si alloy at 1000 °C

reactive system is the contact angle on the reaction product, i.e. on SiC. This angle, measured by Ferro and Derby [15] at 1100 °C using sintered SiC, was found to be equal to 26° both for α- and β-SiC. In the present study contact angles close to 30° were achieved after 6500 s at 1000 °C (see section "Effect of carbon structure").

In order to reveal the microstructure of SiC growing at the interface close to the triple line, three wetting experiments were interrupted, by cooling rapidly (by more than 100 °C/min), after 60 and 600 and 1800 s. After removing the droplets by dissolution, the samples were observed with SEM. Figure 2b is a top view of the interface surface in an area belonging to the quasi-linear stage ($t = 600$ s). The microstructure is columnar and the growth direction of SiC-faceted dendrites is towards the triple line. This can be easily explained by the fact that in the triple line region, where the liquid has direct access to the solid substrate, dissolution of the substrate into the alloy provides the carbon needed for dendrite growth. This microstructure is very different from that at $t = 60$ s where the SiC layer consists of small, micronic sized, particles (Fig. 2a). These results confirm the findings of Dezellus et al. [16] that, in reactive wetting, after a transient stage at the beginning of spreading, where the microstructure is predominantly equiaxed, a steady state is established featuring quasi-linear wetting associated with columnar growth. As for the microstructure of the reactive zone corresponding to the last, very slow final stage of spreading, this is presented in Fig. 2c. This zone was revealed, thanks to receding of the triple line produced during cooling. Figure 2c shows the transition of SiC microstructure from zone B (quasi-linear regime) to zone C as well as the formation in front of the triple line of a film a few microns wide (zone D). Figure 3 shows that both zone C and the film (zone D) consist of very small particles, a few tens to a few hundreds of nanometres in size. X-ray microanalysis of the film reveals the presence of Al and Si together with carbon. The film is either a mixture of Al and Si carbides or more probably a ternary carbide formed by diffusion of Al and Si from the droplet over the carbon-free surface. When the liquid alloy comes into contact with the film, its composition must change to SiC, because neither Al_4C_3 nor ternary carbides of Al and Si are stable in contact with an Al–25 at.% Si alloy at 1000 °C [7].

The quasi-linear reactive stage was modelled in [16, 17] for the case where the spreading rate is controlled by the process of atom transfer occurring at the substrate/liquid alloy interface close to the triple line. The following equation was derived for the relation between the spreading rate U and the cosine of the instantaneous contact

$$\frac{U}{F(\theta)} = k\left(\frac{3V}{\pi}\right)^{1/3}(\cos\theta_E - \cos\theta) \qquad (1)$$

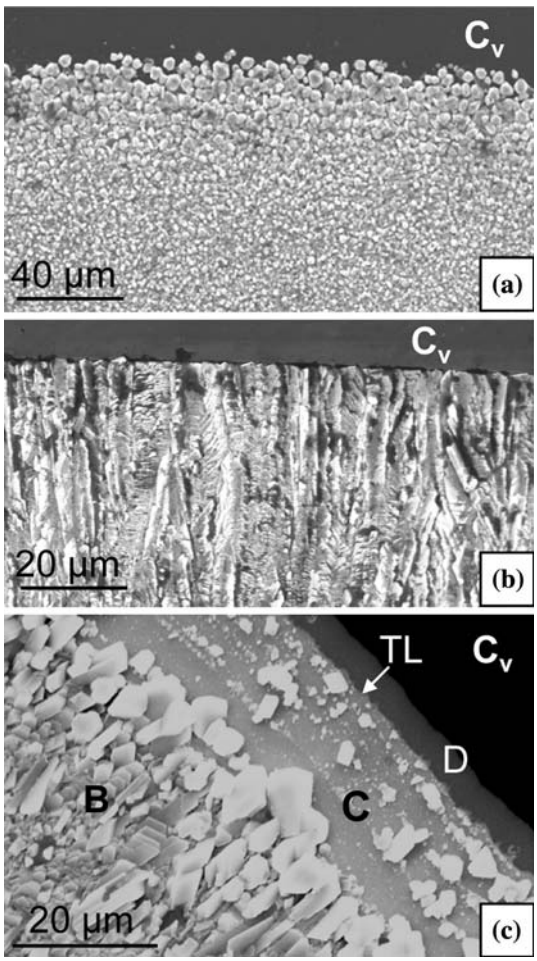

Fig. 2 Top view of the reaction layers close to the triple line for the experiments interrupted after 60, 600 and 1800 s of spreading (**a**, **b**, and **c**, respectively). $T = 1000$ °C, vitreous carbon

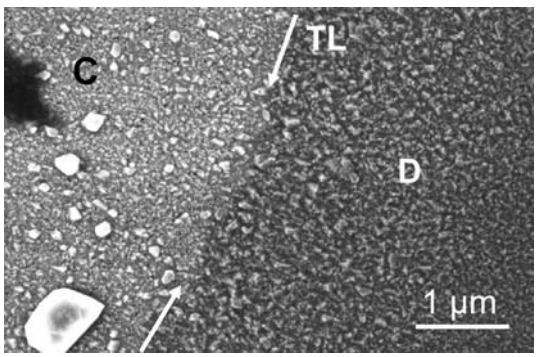

Fig. 3 Top view of the interface showing the transition between the reaction zones C and D for the experiment interrupted after 1800 s of spreading. $T = 1000$ °C, vitreous carbon

with

$$F(\theta) = -\frac{\cos\theta\,(2 - 3\cos\theta + \cos^3\theta) - \sin^4\theta}{\sin\theta\,(2 - 3\cos\theta + \cos^3\theta)^{4/3}}$$

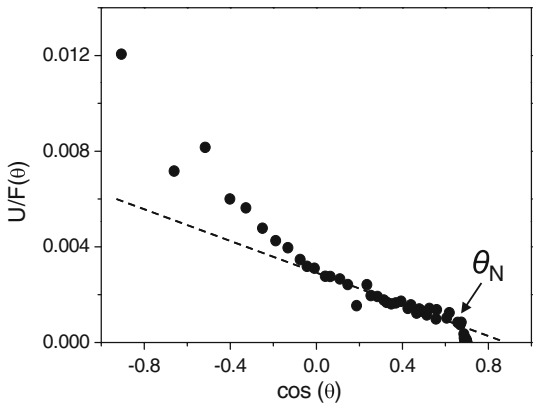

Fig. 4 $U/F(\theta)$ as a function of cos θ for an experiment performed on vitreous carbon with Al–25 at% Si alloy at 1000 °C

V being the volume of the droplet, θ_E the contact angle when the capillary equilibrium is attained and k a constant proportional to the kinetic constant of the dissolution process K_d and to the driving force of the dissolution process $\Delta\mu$. This driving force is equal to the difference between the chemical potential of carbon in the solid and the liquid and is related to the thermodynamic activity of Si in the alloy a_{Si} by the equation:

$$\Delta\mu \approx RT \ln\left(\frac{a_{Si}}{a^{l}_{Si}}\right) \quad (2)$$

where a^{l}_{Si} is the minimum value of Si activity necessary for SiC formation by reaction between Si in the alloy and pure solid carbon. Figure 4 shows a plot of $U/F(\theta)$ as a function of cos θ. The experimental results verify the linear trend predicted by Eq. 1 for contact angles lying between 110° and 45°, i.e. for a domain corresponding to dendritic growth. Extrapolation of the straight line to $U = 0$ gives a value of $\theta_E = 30°$ for the contact angle on SiC which is in good agreement with the experimental value of Ferro and Derby [15].

Spreading kinetics controlled by the atomic transfer process at the substrate/liquid alloy interface close to the triple line implies a high activation energy, i.e. a strong effect of T on the spreading rate U^*, a relatively weak effect of the concentration of the reactive element on U^* as indicated by Eq. 2 and a spreading rate depending on the substrate structure (here carbon).

Interfacial reactivity

The micrographs in Figs. 2 and 3 present the microstructure of the reaction layer close to the triple line *during* the spreading process. The micrographs given subsequently concern exclusively the reaction layer at the centre of the interface (where the interface results from direct contact between the liquid alloy and the carbon substrate) observed at $t > t_F$ (i.e. after a contact time of several tens of minutes.

Figure 5a shows a cross-section of the reaction zone observed after 30 min at 1000 °C. This consists of an apparently continuous layer 3–4 μm thick and of several crystals growing on top of the layer. By increasing the holding time to 60 min, a limited but significant thickening of the layer takes place (layer thickness $e \approx$ 5–6 μm) (Fig. 6a). It can be easily shown, using literature data [18, 19], that grain boundary diffusion of Si or carbon in SiC at 1000 °C is too slow to explain such a thickening. As shown elsewhere [20] thickening of this layer occurs by liquid state diffusion of carbon. Indeed, according to this study, pockets of liquid are formed between the equiaxed layer and solid carbon, which communicate with the outside liquid through pores existing in the equiaxed layer. This enables carbon diffusion to occur from the dissolution

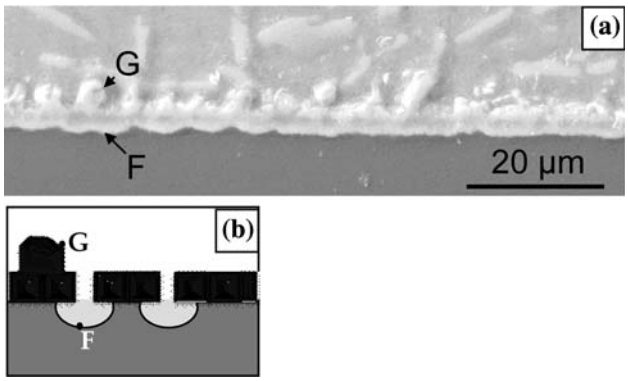

Fig. 5 Cross-section of the reaction layer for an experiment performed for 30 min at 1000 °C with an Al–25 at% Si alloy on vitreous carbon (**a**) and schematic presentation of the reaction layer according to [20] (**b**)

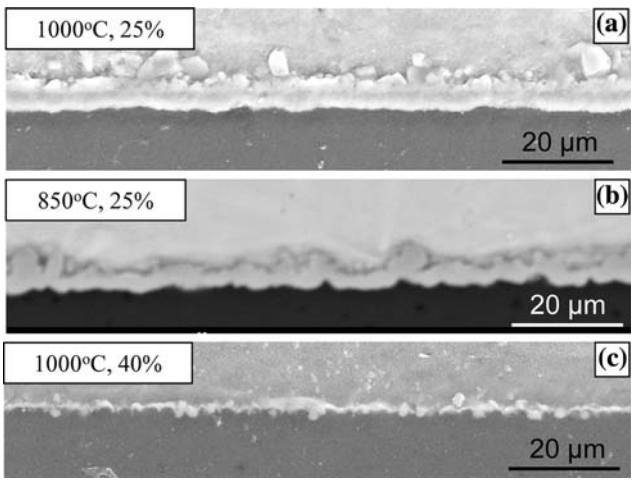

Fig. 6 Cross-sections of the reaction layers in the middle of the drops for experiments performed on vitreous carbon at 1000 and 850 °C with an Al–25 at% Si alloy (**a**,**b**) and at 1000 °C with an Al–40 at% Si alloy (**c**). The holding time is 60 min for all samples

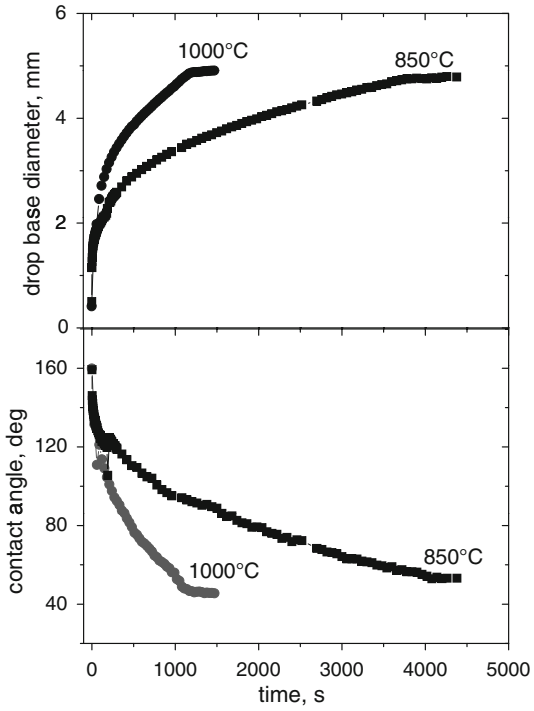

Fig. 7 Effect of temperature on wetting of vitreous carbon by Al–25 at% Si alloy

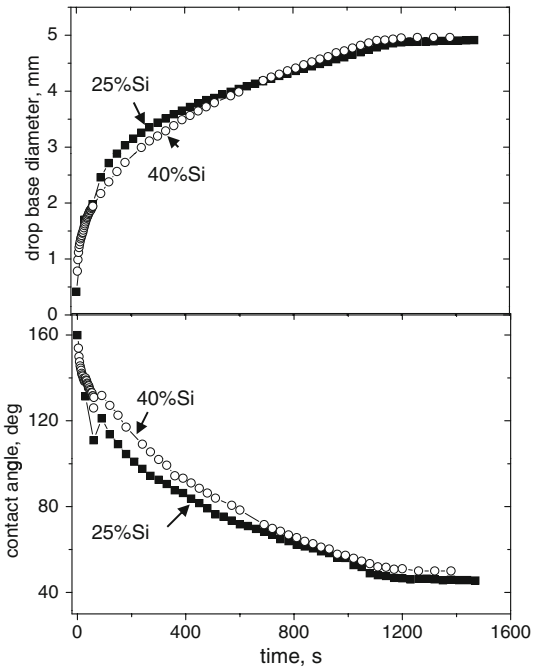

Fig. 8 Effect of Si content on wetting of vitreous carbon by AlSi alloys at 1000 °C

interface (i.e. the solid carbon/liquid layer interface, point F in Fig. 5a) towards the outside liquid where carbon reacts with Si to form SiC (point G).

Effect of temperature

For spreading controlled by the reaction process at the triple line, a strong effect of temperature on the spreading rate is expected. This is confirmed by the results of Fig. 7 showing that a decrease in T of 150° leads to threefold increase in spreading rate U^*. Although it is not possible to calculate an accurate value of activation energy of wetting from only two values, the above results indicate that this energy is high (more than 100 kJ/mol). The effect of T on the thickness e is less pronounced (decrease by a factor of 1.5 (Fig. 6b)), corresponding to an apparent activation energy of diffusion of about 30 kJ/mol. This value is in the range of activation energy of diffusion in liquid alloys [21], thus confirming that the layer growth is controlled by liquid state diffusion.

Effect of alloy composition

The increase in silicon content of the alloy from 25 to 40 at.% has a weak effect on spreading kinetics (Fig. 8). The comparison of U^* values (Table 1) indicates an increase by a factor of 1.25. In order to compare this result with a prediction based on Eq. 2, we have to calculate a^l_{Si},

Table 1 Effect of Si content of AlSi on the spreading rate of the quasi-linear stage U^*

Si content	U* (μm/s)
25 at% Si	0.77
25 at% Si	0.80
40 at% Si	1.00
40 at% Si	1.03

Two experiments per composition were performed at 1000 °C with C_v

the minimum value of Si activity necessary for SiC formation by the reaction

$$(\mathrm{Si}) + \mathrm{C} \rightarrow \mathrm{SiC}$$

where the round brackets mean that Si is in a liquid solution. Then a^l_{Si} is related to the standard Gibbs energy $\Delta G°_f$ of SiC formation from pure graphite and pure molten Si by

$$\Delta G^0_f = RT \ln a^l_{Si}$$

Using the thermodynamic quantities of mixing of AlSi alloys given in [22] in order to calculate the $a_{Si}(x_{Si})$ values and taking for $\Delta G°_f$ the value −62264 J/mol [22], the ratio $\delta = U^*(x_{Si} = 0.40)/U^*(x_{Si} = 0.25)$ is found to be equal to 1.21. Alternatively, taking the value −75573 J/mol for $\Delta G°_f$ given in [23], we find $\delta = 1.16$. Both δ values show that model Eq. 2 predicts a limited effect of alloy

concentration on spreading rate in the quasi-linear stage, in good agreement with the experimental results.

The results on the interfacial reactivity are rather surprising. The increase in Si content not only does not produce an increase in the layer thickness *e* but causes a very significant decrease in this quantity, by a factor of 4–5 (Fig. 6c). Jaquier et al. [6] argued that when the Si concentration in AlSi alloy increases, the carbon concentration in the alloy in metastable equilibrium with solid carbon (point F in Fig. 5b) decreases. This implies a decrease in the driving force of diffusion of carbon from F to G and, as a consequence, a decrease in SiC growth rate.

Effect of carbon structure

As mentioned in section "Spreading kinetics", for spreading controlled by the reaction process at the triple line the spreading rate would depend on the type of carbon substrate. This is confirmed by the wetting curves of Fig. 9 showing that the spreading rate U^* varies in the order $C_v > PC \approx HOPG$ (U^* for C_v is higher by a factor of 2–3 than U^* for PC and HOPG). As argued in [24] for the Al/carbon couple, the transfer of C atoms from the substrate to the liquid is controlled by the breaking of C–C bonds on the substrate surface. This process is affected by the atomic defects in carbon which are more numerous in vitreous carbon than in pyrographite and in HOPG.

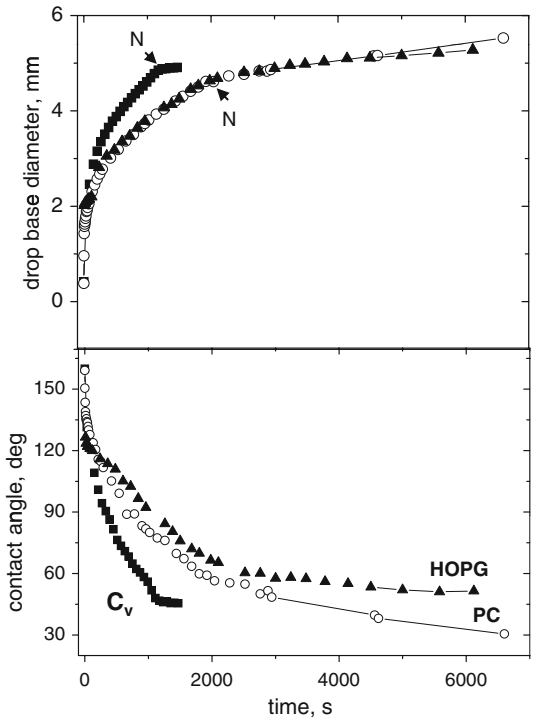

Fig. 9 Effect of carbon structure on wetting of vitreous carbon by Al–25 at% Si alloy at 1000 °C: vitreous carbon (*filled squares*), HOPG (*filled triangles*) and pyrocarbon (*open circles*)

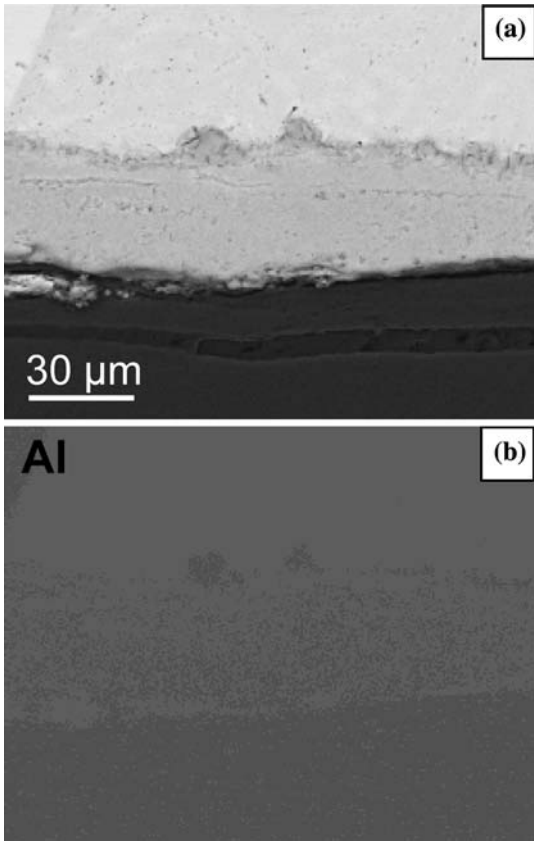

Fig. 10 Cross-section of the reaction layer observed on pyrocarbon after 72 min at 1000 °C with Al–25 at% Si alloy. SEM image **a** X-ray map of Al (**b**)

Figure 10a presents the reaction layer observed for the Al–25 at.% Si alloy with PC at 1000 °C after 72 min. The thickness *e* is 40–50 µm compared to 5–6 µm for C_v. Similarly, a 30 µm thick layer was formed with HOPG after 155 min. Note that the difference in *e* between C_v and HOPG cannot be explained by the differences in the holding time. Indeed, assuming that thickening in C_v follows a parabolic law, the reaction layer in 155 min would be equal to 9 µm, which is still much lower than the 30 µm measured for HOPG. EDS analysis indicates the presence inside SiC of some Al-rich inclusions parallel to the interface (Fig. 10b). It seems that, with PC and HOPG substrates, the alloy penetrates between the graphitic domains bonded only by weak Van der Waals forces, thereby considerably increasing the contact area between the alloy and the carbon material. Note that in a sessile drop experiment performed with pure Si on HOPG, Dezellus et al. [25] observed a progressive decrease in drop visible volume caused by Si penetration between the graphite basal planes.

Conclusions

Wetting dynamics of silicon carbide forming AlSi alloys on carbon substrates is governed by the reaction between Si and carbon. After a transient stage, during which the reaction product microstructure is equiaxed, spreading occurs in two stages. In the first, spreading is controlled by the atomic process at the substrate/alloy interface close to the triple line resulting in quasi-linear spreading and dendritic growth. In agreement with model predictions, the spreading rate in this stage increases strongly with temperature and weakly with Si content in the alloy and is sensitive to the carbon substrate structure. The second spreading regime occurs at low contact angles and with significantly lower spreading rates (order of magnitude). During this stage the moving triple line is preceded by a thin reaction layer a few microns wide. Concerning the reactivity behind the triple line, this is limited by the diffusion of reactive species through the reaction layer. As the processes limiting the two types of reactivity, at the triple line (reflected by the spreading rate) and behind the triple line, are basically different, the effect of parameters such as temperature, alloy composition or again substrate structure on these types of reactivity can be very different.

References

1. Eustathopoulos N, Nicholas M, Drevet B (1999) Wettability at high temperature. Pergamon Materials Series, vol 3. Pergamon, Oxford, UK
2. Hodaj F, Dezellus O, Barbier JN, Mortensen A, Eustathopoulos N (2007) J Mater Sci 42:8071. doi:10.1007/s10853-007-1915-0
3. Howe JM (1993) Intern Mater Rev 388:233
4. Rodrigez-Guerrero A, Molina JM, Rodrigez-Reinoso F, Narciso J, Louis E (2008) Mater Sci Eng A 495:276
5. Rendakova S, Ivantsov V, Dmitriev V (1998) Mater Sci Forum 264:163
6. Jacquier C, Chaussende D, Ferro G, Viala JC, Cauwet F, Monteil Y (2002) J Mater Sci 37:3299. doi:10.1023/A:1016147420272
7. Viala JC, Fortier P, Bouix J (1990) J Mater Sci 25:1842. doi:10.1007/BF01045395
8. Naidich YV, Zabuga VV, Perevertailo VM (1992) Adgeziya rasplavov i payka materialov 27:23 (in Russian)
9. Saiz E, Tomsia AP (2004) Nat Mater 3:903
10. Protsenko P, Kozlova O, Voytovych R, Eustathopoulos N (2008) J Mater Sci 43:5669. doi:10.1007/s10853-008-2814-8
11. Landry K, Eustathopoulos N (1996) Acta Mater 44:3923
12. Bougiouri V, Voytovych R, Dezellus O, Eustathopoulos N (2007) J Mater Sci 42:2016. doi:10.1007/s10853-006-1483-8
13. Dezellus O (2000) PhD Thesis, INP, Grenoble
14. Eustathopoulos N (2005) Curr Opin Solid State Mater Sci 9:189
15. Ferro AC, Derby B (1995) Acta Metall Mater 43:3061
16. Dezellus O, Hodaj F, Eustathopoulos N (2002) Acta Mater 50:4741
17. Dezellus O, Hodaj F, Eustathopoulos N (2003) J Eur Ceram Soc 23:2797
18. Hon MH, Davis RF (1979) J Mater Sci 14:2411. doi:10.1007/BF00737031
19. Hon MH, Davis RF, Newbury DE (1980) J Mater Sci 15:2073. doi:10.1007/BF00550634
20. Voytovych et al, to be published
21. Geiger GH, Poirier DR (1980) Transport phenomena in metallurgy. Adison-Wesley series in metallurgy and materials. Adison-Wesley Publishing Company
22. Kubashevski O, Alcock CB, Spencer PJ (1993) Materials thermochemistry, 6th edn. Pergamon Press
23. Barin I (1995) Thermodynamical data of pure substances, 3rd edn. Weinheim, New York
24. Landry K, Kalogeropoulou S, Eustathopoulos N (1998) Mater Sci Eng A 254:99
25. Dezellus O, Jacques S, Hodaj F, Eustathopoulos N (2005) J Mater Sci 40:2307. doi:10.1007/s10853-005-1950-7